

Revue des Composites et des Matériaux Avancés-Journal of Composite and Advanced Materials

Vol. 35, No. 5, October, 2025, pp. 857-871

Journal homepage: http://iieta.org/journals/rcma

Experimental and Statistical Analysis for Eco-Friendly Self-Compacting Concrete Incorporating Recycled Coarse Aggregate and Nano-Glass Waste



Jumah Musdif Their¹, Oday Ali Azez Altayawi^{2*}

- 1 Anbar Education Directorate, Ministry of Education, Ramadi 31001, Iraq
- 2 Department of Civil Engineering, College of Engineering, Kirkuk University, Kirkuk 36001, Iraq

Corresponding Author Email: odayazez@uokirkuk.edu.iq

Copyright: ©2025 The authors. This article is published by IIETA and is licensed under the CC BY 4.0 license (http://creativecommons.org/licenses/by/4.0/).

https://doi.org/10.18280/rcma.350506

Received: 5 September 2025 Revised: 5 October 2025 Accepted: 26 October 2025

Available online: 31 October 2025

Keywords.

SCC, fresh properties, mechanical properties, NRG, recycled coarse aggregate

ABSTRACT

Sustainable concrete requires high-performance materials that also support resource circularity. The drive toward sustainable concrete innovation necessitates the integration of high-performance materials with circularity in resource use. This study investigates the combined incorporation of nano recycled glass (NRG), derived from post-consumer waste bottles, and recycled coarse aggregate (RCA), obtained from demolition debris, into self-compacting concrete (SCC). The objective was to assess the feasibility of producing eco-friendly SCC by partially replacing cement with 0-3% NRG and substituting natural coarse aggregate with 0%, 50%, and 100% RCA, while maintaining a constant binder content of 550 kg/m³. The mixtures were tested for workability, stability, strength development, and microstructural integrity following standardized procedures. Results revealed that NRG enhanced flowability and compressive strength owing to its fine morphology and pozzolanic activity. Although RCA generally reduced workability and mechanical performance, the inclusion of NRG mitigated these losses, enabling acceptable structural qualities even at full RCA replacement. Overall, the findings confirm that integrating NRG and RCA supports zero-waste and carbonconscious construction practices without compromising essential engineering performance.

1. INTRODUCTION

The management of industrial and construction waste has emerged as a critical global environmental issue [1]. Poorly managed waste contributes to environmental degradation, land scarcity, and resource depletion [2]. Concrete debris accounts for nearly 80% of construction and demolition waste [3]. In the construction sector, sustainable concrete incorporating recycled materials has attracted significant interest as a practical approach to minimizing waste generation and conserving natural resources [4].

Rapid urbanization and infrastructure upgrades have further escalated construction and demolition waste generation, reaching nearly 3 billion tons per year globally [5]. Aggregates constitute more than 70% of concrete's total volume, and their demand continues to grow [6]. A promising solution to improve sustainability in construction is the repurposing of waste concrete into recycled aggregates (RA), which can replace natural aggregates like sand and gravel [7-9]. The use of RA not only decreases landfill dependency but also preserves raw materials. Replacing natural aggregates with RA offers an effective way to reduce environmental impacts while improving resource efficiency and supporting sustainable construction [10].

RA typically exhibits inferior properties compared to

natural aggregates, including lower density, higher water absorption, and greater porosity due to residual mortar adhesion, potentially impacting concrete performance. Studies on recycled concrete aggregates reveal mixed effects on concrete performance. Aljumaili et al. [11] reported that RCA negatively impacts slump flow diameter, T500 flow time, Vfunnel flow time, and L-box passing ability, with the most notable reductions occurring at higher RCA replacement levels (30%). Despite these declines, self-compacting concrete (SCC) containing RCA still met EFNARC specifications for flow and passing ability. Regarding hardened properties, Parthiban and Mohan [12] observed significant reductions in mechanical strength and durability due to RCA's inherent defects and interfacial transition zones (ITZs) [13]. Aljumaili et al. [14] further confirmed that increasing RCA content generally reduces compressive and flexural strength.

Beyond concrete waste, glass waste poses another major environmental threat. As a non-biodegradable material, glass ranks among the most persistent waste types, second only to plastics [15]. Single-use glass products, such as beverage bottles, contribute substantially to municipal solid waste, accounting for about 5% of global waste in 2016 [5]. Incorporating waste glass into concrete production probably offers a sustainable solution to enhance material performance while reducing environmental impact. Research by Lu and

Poon [16] and Lee et al. [17] indicates that waste glass powder reduces the workability of fresh concrete, with finer particles causing more pronounced effects.

Complementary studies by Omran and Tagnit-Hamou [18] reveal that glass powder with particle sizes below 38 µm can significantly improve compressive strength at later ages (more than 90 days) due to enhanced pozzolanic reactivity, while concurrently requiring higher water content to achieve comparable workability to conventional mixes. Recent studies show that finer glass particles exhibit stronger pozzolanic reactivity due to higher surface area and faster silica dissolution in cementitious pore solutions. This improved reactivity manifests in superior long-term strength development [17, 19]. Further supporting this, Aliabdo et al. [20] found that 20% glass powder replacement optimally enhances durability (notably sulfate resistance) while keeping workability loss below 20%. These findings systematically demonstrate the inverse relationship between fresh-state workability and hardened-state performance characteristics in glass-modified concrete systems.

Studies on NRG reveal similar trends, with, Poudel et al. [21] noting reduced slump flow due to increased mix viscosity. Similarly, NRG has been found to extend flow time, suggesting higher viscosity at replacement levels of 10-20% [22]. The L-box test further demonstrates that NRG can decrease the H₂/H₁ ratio, indicating reduced passing ability [23]. Nano glass particles improve compressive strength, reduce shrinkage, and enhance durability in concrete [21, 24-26]. Onaizi et al. [27] reported that nano waste glass can increase compressive strength by up to 26% compared to conventional concrete. Moreover, finer glass particles enhance pozzolanic reactivity, leading to better long-term performance [28]. Recent investigations have further elucidated the influence of NRG on concrete properties.

For instance, Ayub et al. [29] demonstrated that incorporating up to 10% waste glass powder as a partial cement replacement in both ordinary Portland cement and limestone calcined clay cement composites not only enhanced compressive strength but also effectively reduced drying shrinkage, particularly in high-strength mixes. Similarly, Grdić et al. [30] observed a significant increase in compressive strength at 56 days when using ground mixed-color milled waste glass, attributing the enhancement to the formation of additional Calcium-Silicate-Hydrate (C-S-H) gel and a denser concrete matrix. The fresh properties of cement mortars incorporating recycled glass aggregate have been examined by Tuaum et al. [31]. They indicated that increasing recycled glass aggregate content led to a slight decrease in flowability and necessitated adjustments in superplasticizer dosages to maintain desired workability. Collectively, these recent studies corroborate earlier findings on the benefits of NRG in concrete, highlighting improvements in mechanical strength, durability, and resistance to deleterious reactions. The enhanced pozzolanic reactivity of finely ground glass particles plays a pivotal role in these improvements, making NRG a promising supplementary material in sustainable concrete production.

Advancements in concrete technology have introduced innovative materials such as SCC, which was developed in the early 1990s to enhance workability, reduce labor requirements, and improve structural quality [32]. SCC is designed to flow and self-consolidate without vibration, as noted by You et al. [33]. The integration of recycled materials like fly ash and waste glass into SCC formulations further

enhances its sustainability and performance. Given the growing focus on sustainable construction, this study explores the feasibility of using industrial waste materials-including recycled concrete aggregates, waste glass, and fly ash in SCC. The research evaluates their effects on mechanical properties to support eco-friendly construction practices. Despite the growing body of research on RA and waste glass in concrete, several limitations remain. Most prior studies have investigated either RCA or glass waste individually, while their combined influence on the fresh and hardened properties of SCC has not been systematically assessed. Moreover, there is limited experimental evidence on how nano-sized recycled glass can mitigate the well-documented drawbacks of RCA, particularly in mixtures designed for zero-waste construction.

This study addresses these gaps by evaluating the simultaneous incorporation of RCA and NRG into SCC, with a constant binder content to isolate their effects. The research contributes new insights into the synergistic potential of these two recycled materials, demonstrating a practical pathway for producing sustainable concrete mixtures that align with circular economy goals while maintaining the engineering performance required for structural applications.

2. MATERIALS

2.1 Cement, FA and superplasticizer

Ordinary Portland Cement (OPC-Type I), commercially known as ALMASS, was utilized as the main binder. Additionally, low-calcium Class F fly ash (FA), provided from Euro Build in India, was incorporated as a supplementary cementitious material to enhance the sustainability and performance of the SCC-NGRA mixtures. The fineness of the cement used was 340 m²/kg, while the FA exhibited a lower fineness of 290 m²/kg, reflecting the relative specific surface areas of their particles. The specific gravity was 3.15 for the cement and 2.2 for the FA, indicating a notable difference in density that may influence the workability and overall behavior of the SCC mixtures. The chemical compositions of both the OPC and FA were determined through X-ray fluorescence (XRF) spectroscopy, and the results are tabulated in Table 1.

Table 1. Chemical composition of cement and FA determined by X-ray fluorescence

Chemical Composition	Cement	FA
SiO ₂	20.50	43.39
Al_2O_3	4.40	26.27
CaO	61.50	9.55
Fe_2O_3	4.20	3.94
TiO_2	0.13	2.12
P_2O_5	0.08	1.43
MgO	2.60	0.99
K ₂ O	1.36	0.59

The OPC complies with ASTM C150 standards for Type I cement, ensuring consistent quality and performance in concrete applications. Meanwhile, the Class F FA meets the requirements of ASTM C618, characterized by its low CaO content (< 10%) and high silica and alumina content, which contribute to its pozzolanic reactivity.

A superplasticizer based on polycarboxylic-ether formulation with a specific gravity of 1.08 \pm 0.02 and PH-

value of 7 ± 1 was used in all mixes to attain the required slump value for fresh.

2.2 Preparation of nano-recycle glass waste

The accumulation of green glass bottles in landfills necessitated the exploration of sustainable recycling methods, leading to the selection of this waste material for the study. The process of NRG preparation shown in Figure 1. The collected glass fragments underwent thorough cleaning to eliminate contaminants before processing. Initial crushing using an electrically powered primary crusher reduced the particle size to a range of 10-50 mm.



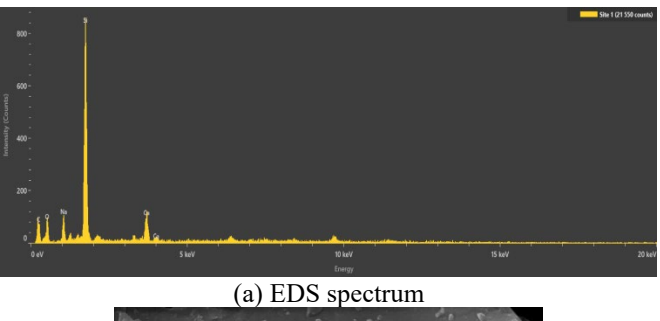
Figure 1. NRG proportion process

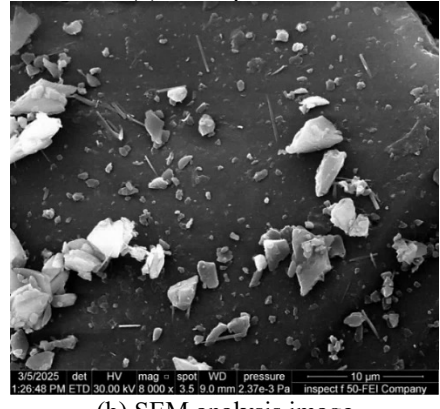
Further refinement of the recycled glass was performed using a laboratory high-energy planetary ball mill (500 mL capacity, stainless-steel jar with zirconia balls), operated in controlled cycles to progressively reduce particle size. The ground material was initially sieved through a No. 50 mesh (300 μm), and the retained fraction was subjected to additional milling. This milling-sieving process was repeated with progressively finer sieves (No. 100 mesh, 150 μm ; No. 200 mesh, 75 μm) until a substantial portion of the powder achieved sub-75 μm size. The final particle size distribution was verified by standard sieving analysis to confirm attainment of the nano-scale range suitable for subsequent use in SCC mixtures.

To optimize the material for use in cementitious systems, the sieved glass powder was dried in a conventional oven at $120\,^{\circ}\mathrm{C}$ for one hour to remove residual moisture, a critical step to prevent interference with subsequent processing. The dried powder was then reclassified using a sieve shaker to isolate particles below 75 μm , ensuring suitability for fine applications. The selected fraction was transferred to a high-energy ball mill, where it underwent intermittent milling cycles of two hours each, interspersed with drying phases at $120\,^{\circ}\mathrm{C}$ to mitigate agglomeration and maintain powder homogeneity. This cyclical grinding-drying process was repeated over a total milling duration of 10 hours, ensuring gradual and uniform particle size reduction. The resulting NRG powder was characterized for consistency and fineness

before incorporation into the experimental concrete mixtures.

Following the production stage, compositional analysis of the NRG was conducted using energy-dispersive X-ray spectroscopy (EDS). The examination revealed a weight composition of 32.6% carbon (C), 24.6% oxygen (O), 5.5% sodium (Na), 31.0% silicon (Si), and 6.3% calcium (Ca). The significant silicon content (31.0 wt.%) confirms silicon dioxide (SiO₂) as the primary phase, consistent with conventional glass composition, see Figure 2(a). The detected sodium (5.5 wt.%) and calcium (6.3 wt.%) concentrations indicate a soda-lime glass structure, commonly employed in commercial glass products. The oxygen content (24.6 wt.%) corresponds stoichiometrically to oxide phases, including SiO₂, Na₂O, and CaO. The significant carbon content (32.6 wt.%) likely originates from surface contamination, residual organic matter during sample preparation, or environmental exposure. Moreover, the prepared NRG exhibited a specific gravity of 2.52.





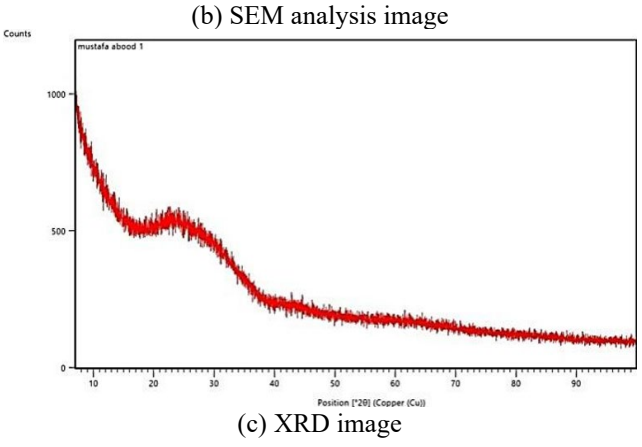


Figure 2. Microstructural characterization of NRG via (a) EDS, (b) SEM, and (c) XRD

Microstructural characterization of the NRG was performed using dry-dispersion laser diffraction (Sympatec RODOS T4.1 Particle Size Analyzer) complemented by scanning electron microscopy (SEM) imaging. Figure 2(b) demonstrates a heterogeneous nanoparticle distribution, featuring irregular sharp-edged flakes, fragmented particles, and occasional needle-like crystals spanning nanoscale to microscale dimensions. This morphology arises from high-energy mechanical grinding and milling processes, which enhance specific surface area and impart unique physicochemical properties.

Table 2. Sieve analysis and physical properties of aggregate

Sieve Analysis	Sieve Size (mm)	Passing (%)		
		Fine Coarse		arse
		Aggregate	Aggregate	
			NCR	RCA
	25.00		100	100
	20.00		98.50	96.20
	12.50		42.70	45.10
	10.00	100	25.30	26.70
	4.75	99.30	2.30	3.10
	2.36	88.20	0.0	0.0
	1.18	67.40	0.0	0.0
	0.60	48.50	0.0	0.0
	0.30	22.30	0.0	0.0
	0.15	6.70	0.0	0.0
Physical	Specific Gravity	2.63	2.65	2.27
Properties	Water Absorption %	1.50	0.50	4.10

The X-ray diffraction (XRD) pattern of the prepared NRG, as shown in Figure 2(c), provides critical insight into the structural nature of the processed material. Utilizing Cu-Ka radiation, the XRD analysis reveals a broad diffraction hump, typically centered around 20°-30° 2θ, which is a well-known signature of amorphous silicate-based materials, including soda-lime glass. The absence of sharp, well-defined peaks indicates that the NRG does not contain any significant crystalline phases. This confirms that the glass retained its amorphous network structure throughout the crushing, milling, and drying processes. The preservation of amorphousness is beneficial when NRG is intended for use as a pozzolanic material or a cementitious additive, as amorphous silica tends to be more reactive in alkaline environments than its crystalline counterparts [34]. On the other hand, the broad hump also indirectly confirms that the high-energy ball milling and drying cycles were effective in reducing particle size without triggering devitrification (crystal formation). This is

crucial: extended or aggressive thermal treatment or improper milling can sometimes cause partial crystallization in glass powders, which would lower their reactivity [35].

2.3 Aggregate

In this study, two types of coarse aggregate were used: Natural Coarse Aggregate (NCA) and RCA. The NCA consisted of crushed gravel with a maximum nominal size of 20 mm, sourced from the Euphrates River in Anbar Province, Iraq, while the RCA was derived from demolition waste of a local building. To maintain experimental uniformity, the RCA was processed to match the particle size distribution of the NCA. This ensured consistent gradation between the aggregates, eliminating particle size variations as a potential factor influencing concrete performance. The fine aggregate consisted of natural sand procured from the Al-Ekhaider quarry, with: maximum particle size, specific gravity, and water absorption of 4.75 mm, 2.63, and 1.5% respectively. The sieve analysis results with gradation limits of Iraqi Standard (IQS No. 45/1984) or ASTM C136/C136M and physical properties of NCA, RCA and fine aggregate are presented in Table 2. In this regard, the sieve analysis results clearly demonstrate compliance with the Iraqi Standard of coarse and fine aggregate sieve analysis (IQS No. 45/1984).

3. MIXTURE PROPORTIONING

SCC contain NRG and RCA (SCC-NGRA) mixtures were formulated with a constant water to cementitious material (w/cm) ratio of 0.35, aiming to maintain high flowability and uniformity while evaluating the effects of recycled components. These mixtures incorporated RCA at replacement levels of 0%, 50%, and 100% by volume of NCA, alongside the inclusion of NRG powder at 0%, 1%, 2%, and 3% by weight of OPC. This design allowed for a comprehensive assessment of the combined influence of RCA and NRG on fresh and hardened properties of SCC-NGRA. A plain reference mixture was also prepared, containing 550 kg/m3 of OPC and FA, with 0% RCA and 0% NRG, to serve as the control. This reference provided a baseline for comparing the performance of modified SCC-NGRA mixtures. In total, twelve distinct SCC-NGRA mixtures were produced, representing all possible combinations of RCA and NRG replacement levels.

Table 3. Mix proportions of SCC-NGRA (kg/m³)

NO.	Code Number	Cement	EA	NRG	Water	Coarse Aggregate		Fine
			FA	NKG		NCA	RCA	Aggregate
1	RCA 0% NRG 0%	412.5	137.5	0.0	192.5	802.2	0.0	805.2
2	RCA 50% NRG 0%	412.5	137.5	0.0	192.5	401.1	343.6	805.2
3	RCA 100% NRG 0%	412.5	137.5	0.0	192.5	0.0	687.2	805.2
4	RCA 0% NRG 1%	407.0	137.5	4.1	192.5	802.4	0.0	805.4
5	RCA 50% NRG 1%	407.0	137.5	4.1	192.5	401.2	343.7	805.4
6	RCA 100% NRG 1%	407.0	137.5	4.1	192.5	0.0	687.3	805.4
7	RCA 0% NRG 2%	401.5	137.5	8.0	192.5	802.6	0.0	805.6
8	RCA 50% NRG 2%	401.5	137.5	8.0	192.5	401.3	343.8	805.6
9	RCA 100% NRG 2%	401.5	137.5	8.0	192.5	0.0	687.5	805.6
10	RCA 0% NRG 3%	396.0	137.5	11.9	192.5	802.9	0.0	805.9
11	RCA 50% NRG 3%	396.0	137.5	11.9	192.5	401.5	343.9	805.9
12	RCA 100% NRG 3%	396.0	137.5	11.9	192.5	0.0	687.8	805.9

Each mixture was labeled systematically to reflect its composition. For example, the designation

"RCA50%NRG2%" identifies the mixture that includes 50% RCA and 2% NRG by weight of OPC. This naming

convention ensures clarity in result interpretation and discussion. To ensure uniform flow characteristics across all mixes crucial for SCC-NGRA performance superplasticizer dosages were carefully adjusted based on preliminary trials, compensating for the reduced workability typically associated with RCA and fine glass particles. All mixtures were prepared following standardized procedures, and their complete proportions, including binder content, aggregate gradation, and admixture dosages, are detailed in Table 3.

4. SAMPLE PREPARATION

A 30-liter laboratory mixing pan was employed for the preparation of all concrete mixtures, adhering to a standardized batching and mixing protocol. Initially, RCA, NCA, and fine aggregate were introduced into the mixer. Following homogenization, the binder components-OPC, FA,

and NRG were incorporated. Approximately one-third of the total mixing water was then gradually added, with mixing continued for an additional minute. Subsequently, the remaining water and high-range water-reducing admixture (HRWRA) were introduced, followed by three minutes of continuous mixing. The mixture was then allowed to rest for two minutes before undergoing a final two-minute mixing cycle to ensure uniformity. The slump flow diameter of the SCC was designed to comply with EFNARC (2005) guidelines, targeting a range of 720 ± 20 mm. Trial batches were cast for each mixture type, with HRWRA dosages adjusted to achieve the specified slump flow. Once the workability of the SCC-NGRA was confirmed, the mixture was cast into molds (cylinders, cubes, and beams) without any compaction, as its self-weight ensured complete filling of voids. All specimens were demolded 24 hours after casting and subsequently cured in a temperature-controlled water tank until testing, see Figure 3.

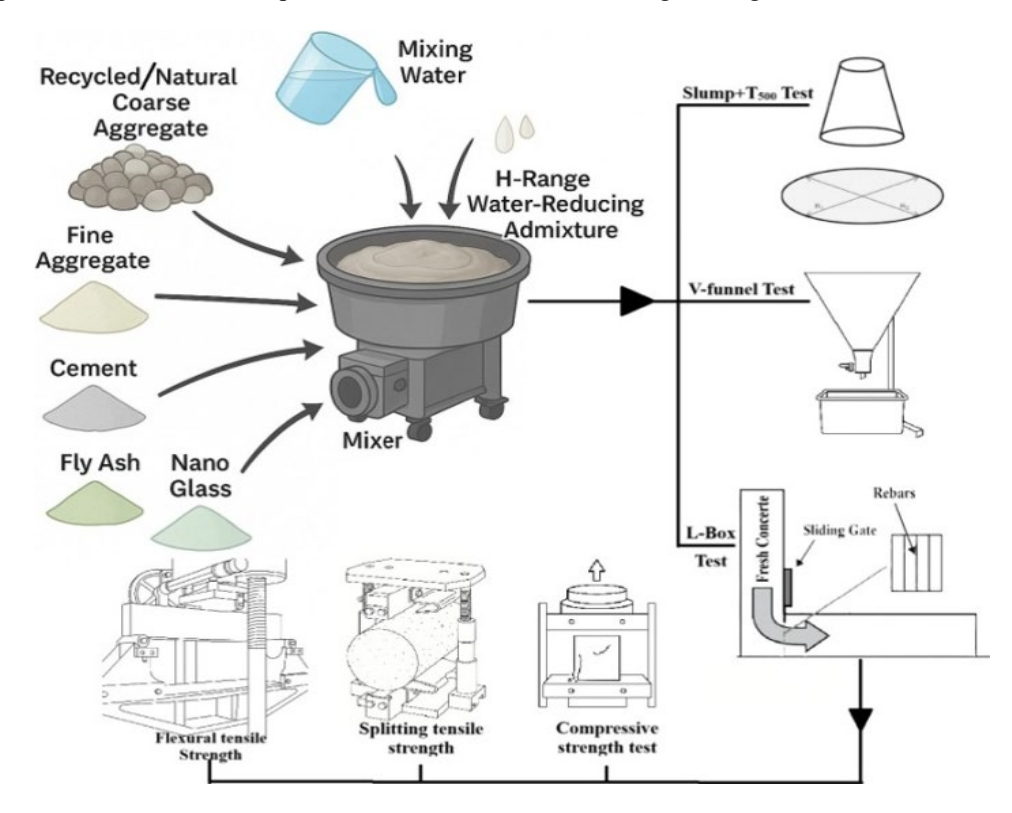


Figure 3. Clarify mixing of SCC-NGRA production

The experimental workflow is effectively summarized in Figures 1 and 3. Figure 1 illustrates the sequential preparation of nano-recycled glass (NRG), while Figure 3 depicts the mixing, casting, and curing stages of SCC-NGRA. Together, these figures provide a visual representation of the entire methodology, serving the same purpose as a conventional flowchart and ensuring transparency of the process.

5. TEST PROCEDURE

5.1 Integrated workability assessment of self-consolidating concrete

The rheological properties of freshly mixed SCC-NGRA were evaluated through a comprehensive suite of standardized workability tests, including slump flow diameter, T500 flow time, V-funnel viscosity, and L-box passing ability

measurements. The slump flow test served as the primary indicator of filling ability, conducted by filling a standard cone (300 mm height, 200/100 mm top/bottom diameters) with uncompact SCC-NGRA and measuring the resulting spread diameter after cone removal (Figure 4(a)). Consistent with EFNARC (2005) guidelines, target slump flow values were maintained at 720 ± 20 mm, while the T500 time - the duration for concrete to reach 500 mm spread - provided complementary viscosity assessment. Visual monitoring during testing further enabled qualitative evaluation of mixture stability and segregation potential, with results categorized into three flow classes to ensure compliance with placement according to BS EN 206:2013 + A1:2016 guidelines requirements [36].

The V-funnel test quantitatively evaluated the concrete's ability to flow through confined spaces, and reinforced congested areas with measured flow time (complete emptying duration) serving as a proxy for viscosity. Following ASTM

C1611/C1611M protocols, the test apparatus was filled with SCC-NGRA and the bottom trapdoor was released to initiate flow (Figure 4(b)). While not a direct rheological measurement, the combined interpretation of V-funnel times (classified per EFNARC 2005) and T500 results provides indirect quantitative assessments of flow resistance, enabling comparative evaluation of SCC-NGRA mixtures. This dual-parameter approach provided critical insights into the SCC-NGRA performance under simulated field conditions, particularly regarding its capacity to navigate congested reinforcement without segregation [37].

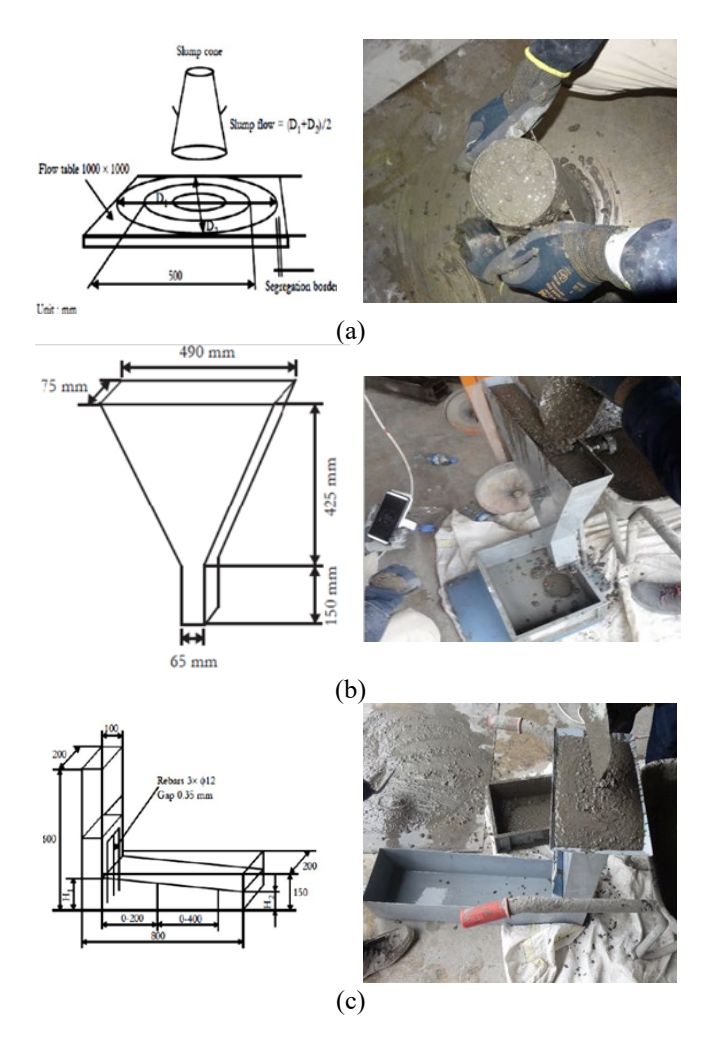


Figure 4. Graphic illustration of dimensions (left) and inprogress flow measurement (right) of (a) slump flow cone, (b) V-shaped funnel, and (c) L-box apparatus

Passing ability was rigorously assessed using an L-box apparatus with three vertically spaced rebars (12 mm diameter, 60 mm spacing) obstructing the gate opening between vertical and horizontal sections (Figure 4(c)). The testing procedure involves filling the vertical section with freshly mixed SCC-NGRA, after which the gate is raised to allow concrete flow into the horizontal section through the obstructions created by the reinforcing bars. Upon cessation of flow, the concrete heights are measured at two critical locations: immediately behind the gate (H_I) and at the end of the horizontal section (H_2) . An H_2/H_I ratio approaching 1.0 indicates superior passing ability, demonstrating the mixture's capacity to flow through congested reinforcement without segregation. As reported in EFNARC (2005) and ASTM C1621/C1621M, thresholds of $H_2/H_I \ge 0.8$ were maintained to ensure adequate

performance in structural applications with dense rebar configurations.

5.2 Mechanical properties evaluation

The mechanical performance of SCC-NGRA was systematically evaluated through compressive, tensile, and flexural strength testing following standardized procedures. In this context, for each mechanical test (compressive, splitting tensile, and flexural), three specimens (n=3) were prepared and tested at each curing age, and the average values are reported.

For compressive strength assessment, 100 mm cubic specimens were cast and tested in accordance with ASTM C39 [38]. Three specimens from each mixture were evaluated at 28 and 90 days using a 3000 kN capacity Universal Testing Machine (CONTROLS Automax, Italy. The failure load was recorded under controlled uniaxial loading at a constant rate, with compressive strength calculated as the mean value of three specimens at each testing age, derived from the maximum load-to-cross-sectional area ratio.

The splitting tensile strength was determined according to ASTM C496 [39] using cylindrical specimens $\emptyset100\times200$ mm, tested on the same 3000 kN capacity Universal Testing Machine (CONTROLS Automax, Italy) equipped with a splitting tensile loading device. The testing configuration involved horizontal placement between compression platens with longitudinal line loading until failure. In this study, the tensile strength of SCC-NGRA was calculated using Eq. (1) as follows:

$$f_{ct} = \frac{2P}{\pi \times L \times D} \tag{1}$$

where, P represents peak load, L denotes cylinder length, and D indicates diameter. As with compressive testing, triplicate specimens were evaluated at 28 and 90 days, with results averaged to ensure statistical reliability.

Flexural performance was characterized using $100 \times 100 \times 400$ mm prismatic specimens in accordance with ASTM C78 [40], tested after 90 days of curing on a 3000 kN capacity Universal Testing Machine (CONTROLS Automax, Italy) under third-point (four-point) loading configuration. The modulus of rupture (f_b) was computed from three specimens using Eq. (2).

$$f_b = \frac{P \times L}{b \times d^2} \tag{2}$$

where, L signifies support span length (300 mm), b specimen width (100 mm), and d depth (100 mm). This configuration provided critical data on the SCC-NGRA's tensile performance under bending stresses, complementing the uniaxial test results. Furthermore, error bars in the graphical results represent standard deviations calculated from triplicate specimens. Coefficients of variation were checked according to ACI 214R-11 guidelines to ensure statistical reliability of the data.

6. RESULTS AND DISCUSSIONS

This section reports the experimental investigation of SCC-NGRA mixtures and interprets the relevance of the obtained

results in the context of sustainable concrete development.

6.1 Fresh properties

In order to characterize the fresh properties of SCC-NGRA, standard procedures were applied, including the determination of slump flow diameter, slump flow time, V-funnel time, and L-box ratio.

6.1.1 Slump flow and workability

An ideal SCC-NGRA mix should exhibit excellent flowability and the ability to pass through congested reinforcement without blockage. Additionally, it must maintain a homogeneous distribution of aggregates while demonstrating high resistance to segregation. These properties are typically assessed through standardized testing procedures [41, 42]. Depending on the intended application, SCC-NGRA performance requirements can be selected from key fresh-state properties (i.e., flowability) and further defined by specific classification thresholds or target values, as outlined in Table 4 [43]. In this study, the inclusion of RCA at 0%, 50% and 100% replacement levels, along with NRG at 0%, 1%, 2%, and 3%, revealed distinct trends across key fresh state parameters - namely slump flow diameter, V-funnel time, slump flow time (T500), and L-box height ratio.

As can be seen in Figure 5, the control mixture exhibited a slump flow diameter of 730 mm, which falls within Class SF2 according to BS EN 206:2013 + A1:2016 guidelines [43], suitable for elements with normal reinforcement congestion. Replacing natural aggregate with 50% and 100% RCA reduced the flow diameter to 725 mm and 715 mm, mainly due to the rough surface and irregular shape of RCA, which increases inter-particle friction and lowers mix lubricity. These observations are consistent with findings reported by Güneyisi et al. [44], who noted similar decrements in flow diameter with increasing RCA levels due to altered rheological response under low shear conditions. NRG incorporation further influenced the flow characteristics. Mixtures with 1% and 2% NRG exhibited minor reductions in flow, while 3% NRG mixtures marked a noticeable decline, with flow values approaching the lower boundary of SF2 classification. The angular morphology and high surface area of NRG particles promote water absorption and increase internal friction, contributing to reduced spread ability. This behavior parallels the observations by Assaad and Khayat [45], who linked fine pozzolanic filler addition with lower workability in SCC due to water demand escalation.

Table 4. Classification of SCC-NGRA properties (slump flow, viscosity, and passing ability) according to BS EN 206:2013+A1:2016 guidelines

Test	Property	Class
Slump flow diameter	Slump Flow	SF1: 550 - 650 mm
		SF2: 660 - 750 mm SF3: 760 - 850 mm
Slump flow time	Viscosity	VS1: < 2.0 s
		$VS2: \ge 2.0 \text{ s}$
V-funnel time	Viscosity	VF1: < 9.0 s
		VF2: 9.0 - 25.0 s
		VF2: 9.0 - 25.0 s
L-box	Passing ability	PL1: ≥ 0.80 with
L-00X		two rebar
		$PL2: \ge 0.80$ with
		three rebar

Simultaneous use of RCA and NRG caused a greater reduction in flowability than when each was added alone (Figure 5). For example, while the fraction of 100% RCA reduced flow diameter by about 2.1% relative to the control, and using 3% NRG alone led to decreased flow diameter by about 2.7%, the combined 100% RCA 3% NRG mixture further decreased flowability by about a 4.1%. This trend suggests a synergistic effect, where the adverse impact of RCA on mix lubricity is amplified by the fine, high surface area NRG particles that further absorb mixing water due to its pozzolanic surface reactivity and restrict cement paste movement. Mechanistically, this interaction can be attributed to the dual increase in internal friction: RCA contributes macro-scale friction due to its angularity and rough texture, while NRG particles influence micro-scale rheology by thickening the cementitious matrix. As a result, the paste's ability to effectively coat and separate aggregate particles diminishes, thereby restricting outward flow during slump testing. This compounded effect corroborates the rheological behavior reported by Zhang et al. [46], who observed that hybrid substitution with recycled and nanostructured materials often demands higher plasticizer dosages to maintain baseline workability. On the other hand, the complex interaction between RCA and NRG highlights the need for rheological fine tuning in mixes targeting sustainability through dual replacement strategies. As demonstrated in a recent study by Mohseni et al. [47], the combined use of recycled and nanomaterial-based modifiers introduces unique challenges in maintaining flow class compliance while also targeting durability and performance metrics. Notably, the reduction in slump flow across mixed RCA and NRG combinations still kept the values within the SF2 classification.

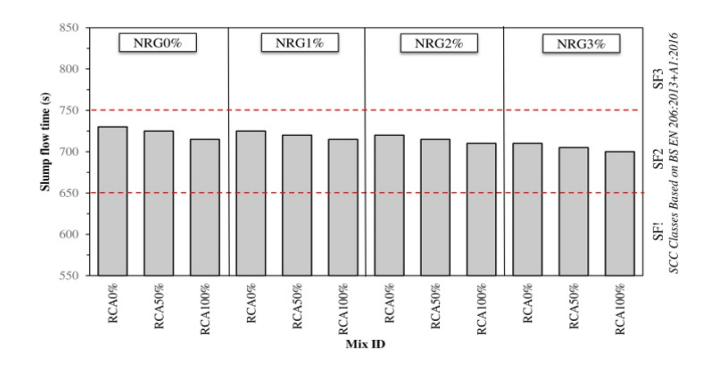
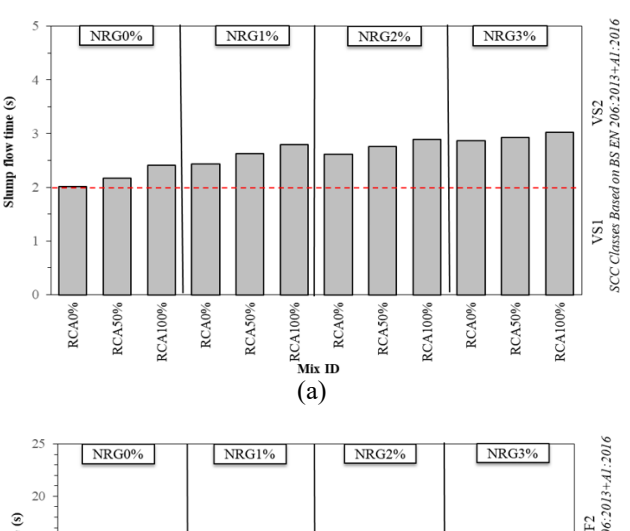


Figure 5. Slump flow diameter of SCC-NGRA mixtures with and without RCA and NRG modification

6.1.2 Viscosity indicators

The results of T500 time (indicative of flow rate) and Vfunnel time are presented in Figures 6(a) and (b), respectively. As shown in Figure 6(a), the T500 time increased progressively with higher RCA and NRG content. Control mixture T500 was recorded at 2.01s, while mixes made with 100% RCA and 3% NRG reached up to 3.02 s, reflecting increased viscosity. On the same line, Figure 6(b) shows Vfunnel time followed a similar trend, increasing from 6.51 s in the control mixture to 11.0 s in the RCA 100% NRG 3% mix. These findings suggest that the combined inclusion of RA and nano additives increases flow resistance, particularly due to the cumulative effect of surface roughness and particle fineness. This response is primarily rooted in the rheological incompatibility introduced by dual-scale heterogeneity: RCA disrupts uniform particle packing and fluid film continuity, while NRG alters paste rheology through microstructural densification. Together, they hinder flow by limiting particle dispersion and reducing lubrication. Such dual-material interactions were also documented by Liu et al. [48], who noted a nonlinear rise in plastic viscosity when coarse recycled particles were paired with mineral fines exhibiting high surface activity. Moreover, a subtle but notable shift in the relative contribution of NRG becomes apparent when RCA levels are high. At 100% RCA, the incremental addition of NRG (from 1% to 3%) yields sharper increases in both T500 and V-funnel times compared to mixes without RCA. This suggests that NRG's influence is amplified in coarse, high-void frameworks, where paste continuity is already compromised. It highlights the importance of mix synergy analysis rather than isolated component optimization in sustainable SCC-NGRA design.

According to BS EN 206:2013+A1:2016 guidelines, these T500 and V-funnel time values correspond predominantly to higher viscosity classifications, necessitating careful admixture tuning to maintain acceptable workability. Notably, even at elevated NG dosages of current study, the mixes remained within functional viscosity limits lower than 12 s for V-funnel, ensuring usability for vertical and horizontal placements. Recent literature also supports this trend; Altayawı et al. [49] emphasized that fine pozzolans, while enhancing long-term performance, often reduce flow speed and necessitate mix optimization.



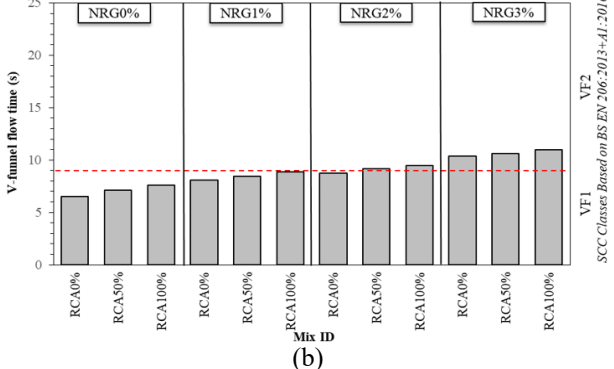


Figure 6. Time-dependent rheological characteristics of SCC-NGRA mixtures: (a) T₅₀₀ and (b) V-funnel test results

6.1.3 Passing ability

The L-box test, which assesses passing ability by simulating reinforcement conditions, showed a consistent decrease in the H_2/H_1 ratio as the content of RCA and NRG increased (see Figure 7). The control exhibited near ideal flow (0.99), whereas the 100RA30NG mixture dropped to 0.86. All mixes, however, remained above the minimum threshold of 0.80

prescribed by BS EN 206:2013 + A1:2016 guidelines confirming adequate passing capacity. In this regard, such trend can be attributed to a dual-phase hindrance effect: RCA imposes geometric blockages due to its angularity and nonuniform size, while NRG thickens the interstitial paste, diminishing the ability of aggregates to reorient and move freely during narrow passage flow. The compounding nature of these factors restricts the mixture's ability to pass through reinforcement simulations without segregation or blockage. These findings align with observations made by Liu et al. [48], highlighted the trade-off between pozzolanic enhancement and passing ability in nanomaterial-modified SCC. Similarly, Altayawı et al. [49] reported a decline in the passing ability of ternary SCC mixes incorporating RA and nano-silica blends.

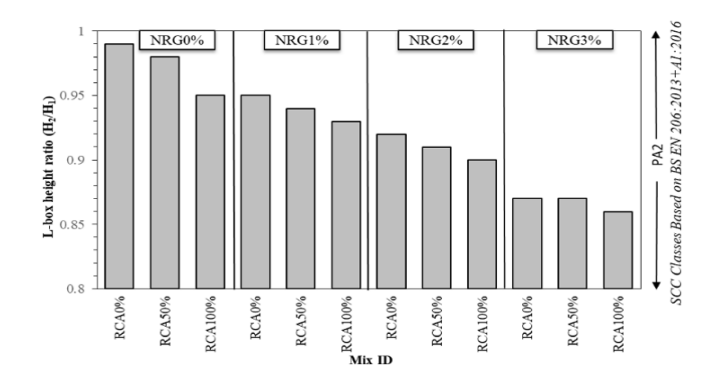


Figure 7. Variation of L-box height ratio for SCC-NGRA mixtures

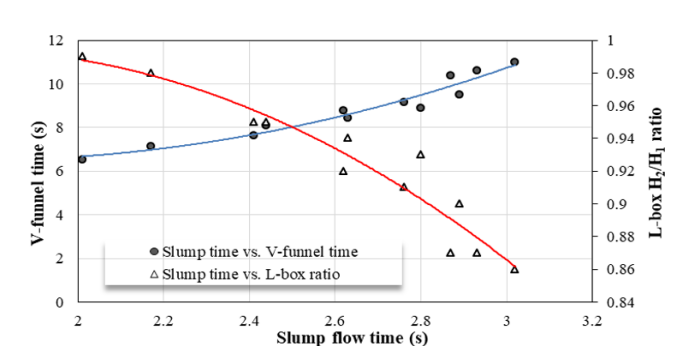


Figure 8. Integrated assessment of viscosity and passing ability in SCC-NGRA: correlation between T₅₀₀, V-Funnel time, and cc ratio

6.1.4 Flow-viscosity-passing correlations

To gain deeper insight into the interdependency of freshstate parameters, a composite figure was developed to illustrate the relationship between T500, V-funnel flow time, and H2/H1 ratio (Figure 8). The plotted data reveal a clear trend: increasing T500 correlates with a simultaneous rise in V-funnel time and a gradual decline in L-box ratio across all mixtures. This tri-directional interaction underscores a shared rheological underpinning where higher internal viscosity whether induced by RCA angularity or NRG powder fineness slows flow and restricts movement through confined spaces. Notably, mixes containing both high RCA and NRG levels cluster toward the higher end of the V-funnel axis and the lower end of the L-box axis, reflecting the most significant resistance to flow and obstruction in passing. The inverse trend between L-box and the other two parameters emphasizes the sensitivity of passing ability to changes in viscosity and yield stress, as thicker pastes impede aggregate mobility under restricted conditions. Despite these reductions, all mixtures remained within the performance thresholds prescribed by BS EN 206:2013+A1:2016, affirming their suitability for structural applications with careful proportioning. The combined figure thus provides a compact yet comprehensive visual synthesis of how modifications to material composition affect flow characteristics, aligning with findings reported in recent multivariable SCC rheology study by Wang et al. [50].

To further elucidate the rheological behavior of the modified SCC-NGRA mixtures, a correlation plot was developed linking slump flow diameter with V-funnel time and H₂/H₁ ratio (Figure 9). The resulting relationships illustrate that as slump flow diameter decreases, V-funnel time increases, indicating a consistent reduction in flowability accompanied by a rise in mix viscosity. Concurrently, the H₂/H₁ ratio trends downward, reflecting diminished passing ability. This inverse correlation suggests that mixes with limited spread ability tend to resist flow under gravity and are less capable of navigating congested formwork, likely due to paste stiffening and aggregate interlock.

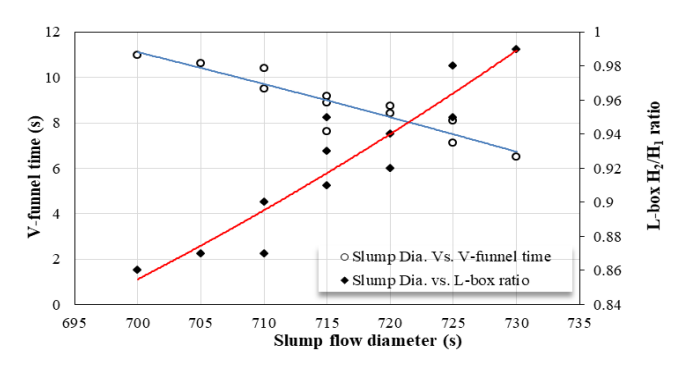


Figure 9. Relationship between flowability, viscosity, and passing ability in SCC-NGRA

This combined plot effectively demonstrates the codependence of fresh-state properties in SCC-NGRA systems incorporating RCA and NRG powder. The decrease in slump diameter is accompanied by reduced mobility of the concrete, indicating that the mix becomes more resistant to movement. This is likely due to the combined effects of the rough surface texture of the RCA, which increases internal friction, and the fine particles of NRG powder, which make the paste denser and less able to flow freely around the aggregates. This graphical analysis aligns with findings by Lee et al. [17], who emphasized the necessity of multi-parameter assessment when designing SCC for hybrid material systems with different replacement levels.

6.2 Hardened properties

The mechanical response of the investigated SCC-NGRA mixtures was evaluated in terms of compressive strength, splitting tensile strength, and flexural strength (modulus of rupture). In addition to direct experimental testing, the study further explored the predictive reliability of existing international models and proposed regression-based correlations. Comparative assessments were performed across all strength parameters to highlight the influence of mix modifications and substitution levels.

6.2.1 Compressive strength development

The compressive strength of all concrete mixtures was evaluated at 28 and 90 days, and the results are presented in

Figure 10. The control mixture reached 39.31 MPa at 28 days and 47.41 MPa at 90 days. Incorporating RCA and supplementary cementitious materials led to notable variations in strength development. For instance, the mixture containing 50% RCA showed a reduction in 28-day strength by approximately 11.9% compared to the control, which is attributed to the weaker ITZ and higher porosity typically associated with RCAs. However, extending the curing age to 90 days mitigated this reduction, indicating a positive longterm pozzolanic contribution from the additives. The general trend suggests that the compressive strength of mixtures incorporating RCA and NRG improves with curing time, progressively narrowing the performance gap with the control mixture. This enhancement can be attributed to the continued hydration of unreacted cement particles and the progressive densification of the matrix. The finely ground glass, acting as a pozzolanic material, reacts with calcium hydroxide to form additional C-S-H, a secondary product which contributes to filling micro-voids and refining the pore structure [51]. This effect becomes more apparent with increasing NRG content, as the additional C-S-H enhances internal packing and strengthens the ITZ [52]. The positive impact is particularly noticeable at later ages, highlighting the long-term reactivity and microstructural benefits provided by NRG.

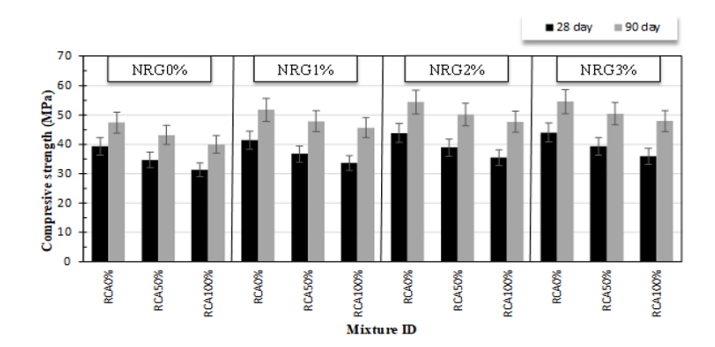


Figure 10. Development of compressive strength in RCA, NRG modified SCC-NGRA. Variability indicated by ACI 214R-1, based error bars. Normalized 28 and 90 days deviations (%) are labeled

Incorporating CV-based error bars enhances the clarity and technical reliability of the data by quantifying inherent testing uncertainty and supporting the visual comparison of mix performance. It enables researchers and practitioners to discern whether observed differences between mixtures are likely due to material modifications or fall within acceptable experimental variability. Furthermore, such estimation allows for benchmarking the quality control level of the mixes and reinforces the reproducibility of results, which is critical for both academic validation and field application. Error bars shown in Figure 10 were calculated following the guidelines of ACI 214R-11 [53, 54], based on an assumed CV of 7.5%, which is appropriate for concrete strengths within the 35-55 MPa range. In addition, the normalized values that represent the percentage deviation from the control mixture are marked above 28 and 90 days. These values serve as a critical lens to assess the influence of the incorporation of RCA and NRG on mechanical performance. At 28 days, a clear reduction in compressive strength was observed in the mixtures containing RCA. The 50% RCA and 100% RCA mixtures exhibited strength losses of approximately 11.9% and 20.3%, respectively, in comparison to the control. This decline can be attributed to the inherent porosity and weaker ITZs commonly associated with RCA. However, the incorporation of NRG demonstrated a compensatory effect. The 1% NRG mixture exceeded the control's performance by 5.3%, indicating enhanced hydration and matrix refinement due to pozzolanic activity. Moreover, the hybrid mixture (50%RCA1%NRG) achieved a more moderate reduction of 6.4%, showcasing the synergistic interaction between partial RCA replacement and NRG supplementation. At 90 days, the positive trend continued across all formulations. The 50% RCA mixture increased its performance to a percent of 9.0%, while the 100% RCA mixture showed a slight positive deviation of 1.6%. Notably, the mixture with 3% NRG exhibited a 38.7% strength gain, reinforcing the long-term reactivity of NRG. On the other hand, the 100%RCA1%NRG mix exceeded the control mixture, with a deviation of 21.8%, suggesting that prolonged curing allows NRG to fully engage in secondary hydration reactions that contribute to improved packing density and strength.

6.2.2 Splitting tensile strength

The splitting tensile strength results are presented in Figure 11 for both 28 and 90 days curing periods. Overall, tensile performance exhibited more sensitivity to compositional changes than compressive strength, reflecting the higher dependency of tensile failure on microstructural continuity and interfacial quality. At 28 days, mixtures containing RCA exhibited notable reductions in tensile strength relative to the control. For example, the 50% RCA mixture experienced an approximate 12.2% drop, which aligns with the expected decline in tensile capacity due to increased porosity, weaker particle bonding, and potential residual micro-cracks introduced during aggregate recycling [55].

Interestingly, mixtures incorporating NRG demonstrated an improved tensile strength recovery over time. At later curing ages, particularly in specimens containing 2% and 3% NRG, the observed tensile gains suggest the development of a more integrated and cohesive internal structure. This can be attributed to the pozzolanic reactivity of the NRG, which contributes to the formation of additional C-S-H gel that not only densifies the matrix but also bridges microcracks [56, 57]. This crack-bridging effect appears to be especially beneficial under tensile loading conditions, where localized weaknesses can lead to brittle failure. In this regard, there is a strong agreement between the current experimental trends and previous studies that used recycled glass and other pozzolans in the production of conventional concrete. Their results showed that the incorporation of such supplementary cementitious materials confers significant splitting tensile strength benefits to recycled aggregate concrete by tightening its internal structure, especially at the aggregate paste interface, providing agents for micro-crack bridging, and facilitating continued strength development beyond the standard 28 days period [58, 59].

As with the compressive strength results, the error bars depicted in Figure 11 were estimated using a coefficient of variation (CV) of 8.0%, consistent with the variability range recommended by ACI 214R-11 for tensile strength in conventional concrete [53, 54]. These statistical bounds support a more transparent interpretation of data reliability and experimental consistency across all tested mixtures. Integrating CV-based variability into the visualization strengthens the analytical depth, especially when comparing the performance of recycled and modified concretes against the control mix. Moreover, normalized deviation values

annotated above each 28 and 90 days bar serve to highlight the relative performance of each formulation. At 28 days, the 50% RCA mixture showed an 18.4% reduction in tensile strength compared to the control, while 100% RCA exhibited a greater decline of 19.2%. Conversely, the inclusion of 1% NRG alone improved the tensile strength by 4.3%. The hybrid SCC-NGRA mixture, namely 50%RCA1%NRG, demonstrated a moderated reduction of 10.4%, reflecting partial compensation by the pozzolanic effect of NRG. A similar trend was observed at 90 days, where strength gains were recorded across all mixtures, reducing the performance gap with the control. Specifically, the normalized loss for 50% RCA improved to 15.3%, while 100% RCA reduced its deficit to 29.7%. The mix with 3% NRG alone further enhanced its performance, reaching a 15.9% increase over the control, whereas the 50%RCA3%NRG mixture yielded a deviation of 12.4% compared to the reference SCC-NGRA mixture. These findings suggest that long-term curing allows for the progressive reactivity of NRG to manifest more fully, contributing to matrix densification and improved tensile integrity. When combined with CV-derived error bands, this dual-layer visualization approach delivers a balanced view of strength development, uncertainty, and material innovation in sustainable concrete systems.

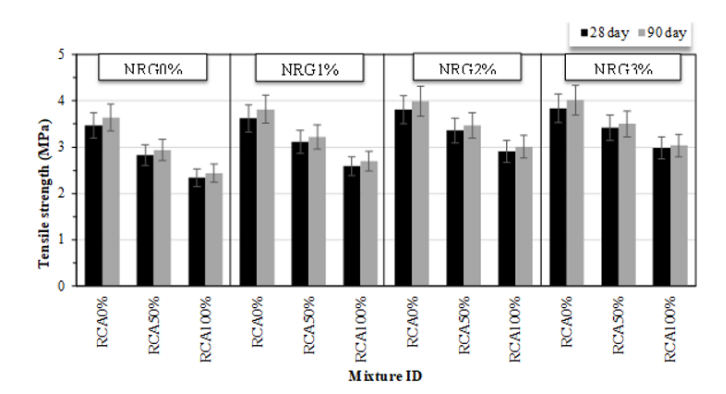


Figure 11. Development of splitting tensile strength in RCA, NRG modified SCC-NGRA. Variability indicated by ACI 214R-11, based on error bars. Normalized 28 and 90 days deviations (%) are labeled

The observed improvements in compressive and tensile strength with NRG addition can be attributed to microstructural modifications revealed by SEM. The nanoglass particles, due to their pozzolanic reactivity and filler effect, contribute to a denser matrix by refining pore structure and reducing voids within the ITZ. This densification enhances load transfer across the paste-aggregate interface, mitigating the common weaknesses associated with RA. Similar mechanisms have been reported by Dahamm et al. [23] and Onaizi et al. [24], who found that finely ground glass powders improved matrix homogeneity and bond strength. Compared with these studies, the present work demonstrates that even at low replacement levels ($\leq 3\%$), NRG can partially offset the reduction in mechanical properties caused by RCA, thereby highlighting its synergistic role in sustainable SCC production.

6.2.3 Flexural tensile strength

Flexural tensile strength is a critical indicator of a concrete mixture's ability to resist bending and crack propagation under transverse loading, making it particularly relevant for structural applications such as beams, pavements, and slabs [60]. Unlike compressive or splitting tensile strength, flexural performance captures the combined influence of matrix cohesion, interfacial bonding, and post-cracking ductility [61]. Assessing this property at later ages is essential for understanding the long-term mechanical behavior of concretes incorporating RA and supplementary cementitious materials, especially in systems where microstructural refinement and delayed pozzolanic activity play a significant role [62].

The evaluation of flexural tensile strength at 90 days offers further insight into the structural integrity of concrete mixtures modified with RCA and NRG. As shown in Figure 12, a descending trend in strength is evident with increasing RCA while NRG incorporation yields notable content. improvements. The control mixture recorded a flexural strength of 3.78 MPa, against which all other mixtures were benchmarked. The 50% RCA and 100% RCA mixtures showed reductions of approximately 22.0% and 40.2%, respectively, relative to the control. These losses are likely attributed to diminished matrix continuity and stress-transfer efficiency due to higher porosity and residual microdefects in RA [54, 63-68]. On the contrary, the 1% NRG mixture outperformed the control, registering a 22.0% increase in flexural strength. The improvement stems from NRG's pozzolanic reactivity, which refines pores, bridges cracks, and strengthens tensile resistance. The hybrid formulation (50%RCA1%NRG) mitigated much of the RCA induced degradation, showing only a 7.4% reduction relative to the control, indicating a partial recovery of tensile integrity through NRG supplementation. To effectively convey these trends, a grouped bar chart with superimposed normalized deviation annotations is recommended. Each bar would represent the average flexural strength, while the normalized percentage differences would be labeled above the bars. Error bars can be added based on an assumed coefficient of CV of 9.0%, which aligns with ACI 214R-11 guidelines for flexural tests in normal-strength concrete [53].

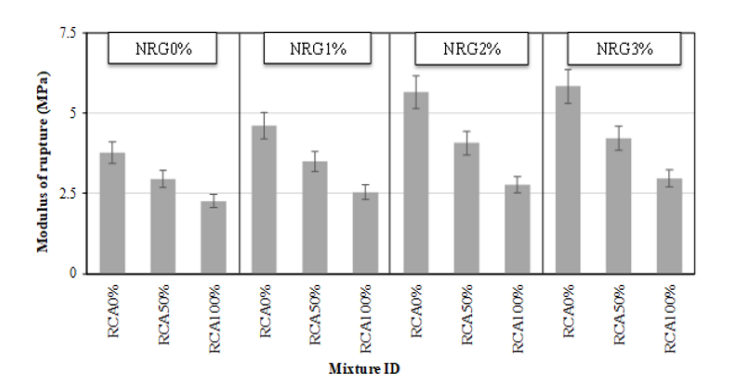


Figure 12. Development of flexural strength in RCA, NRG modified SCC-NGRA. Variability indicated by ACI 214R-11, based error bars. Normalized 90 days deviations (%) are labeled

6.3 Strength correlation and benchmarking

To extend the understanding of mechanical behavior beyond individual strength metrics, this section presents a comprehensive evaluation of 90 days hardened properties through statistical correlation and comparative benchmarking. It is noteworthy that flexural strength was exclusively measured at 90 days; therefore, this section intentionally focuses on 90 days test results only. The evaluated concrete mixtures are all based on SCC-NGRA, which is characterized

by its flowability, high paste volume, and reduced compaction energy requirements actors that may influence mechanical correlations and performance trends.

6.3.1 Correlation of compressive strength with splitting tensile strength and flexural strengths

The relationship between compressive strength and tensilerelated properties is critical for predicting concrete performance. In this regard, splitting tensile and flexural tensile strengths were analytically correlated with compressive strength through regression modeling, enabling the derivation of empirical relationships characterizing the mechanical behavior of the SCC-NGRA mixtures (see Figure 13). A pronounced linear correlation was observed between compressive strength and splitting tensile strength, revealing a strong predictive linkage across the SCC-NGRA mixtures. This trend suggests that compressive strength serves as a reliable indicator of tensile performance, likely due to shared dependence on matrix integrity and internal load distribution mechanisms. The strength correlation is consistent with previous reports in the literature. For example, Şahmaran et al. [64] found similar proportionality between compressive and tensile strength in self-consolidating systems incorporating supplementary cementitious materials. In contrast, the relationship between compressive strength and flexural strength followed an exponential trend. This may reflect the increasingly brittle to ductile transition behavior of SCC-NGRA as compressive strength increases, particularly when nano-sized pozzolanic additives such as NRG are present. The exponential model also highlights the enhanced post cracking performance observed in the strength of SCC-NGRA, corroborating findings by Mustapha et al. [65], who demonstrated similar trends when nano-silica was used to improve flexural capacity. Notably, the higher R2 value for flexural strength correlation implies a more predictable response under bending conditions, possibly due to the beneficial matrix densification and crack-bridging effects imparted by NRG particles. A similar trend was reported by Li et al. [66], who demonstrated that incorporating nano-silica into SCC mixtures enhanced flexural capacity through matrix densification and crack-bridging mechanisms, even when improvements in compressive strength remained modest.

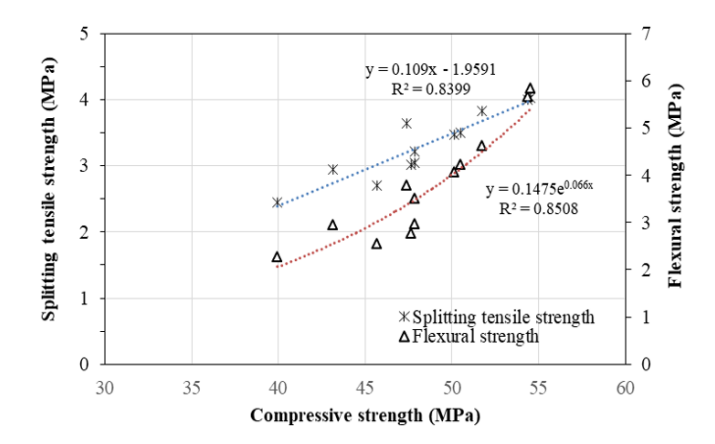


Figure 13. Correlation of compressive strength with splitting tensile and flexural tensile strengths in SCC-NGRA mixtures

Overall, these correlations provide useful predictive tools and validate the composite behavior of SCC mixtures modified with sustainable materials. Their high degree of fit confirms the internal consistency of the experimental data and sets a foundation for engineering level design estimations in future SCC applications.

6.3.2 Normalized mechanical index

To quantitatively benchmark the overall mechanical performance of each SCC-NGRA mixture, a Normalized Mechanical Index (NMI) was developed based on compressive strength, splitting tensile strength, and flexural tensile strength results. Each value was normalized relative to the control, and the NMI was computed as the arithmetic mean of the three normalized parameters (see Figure 14).

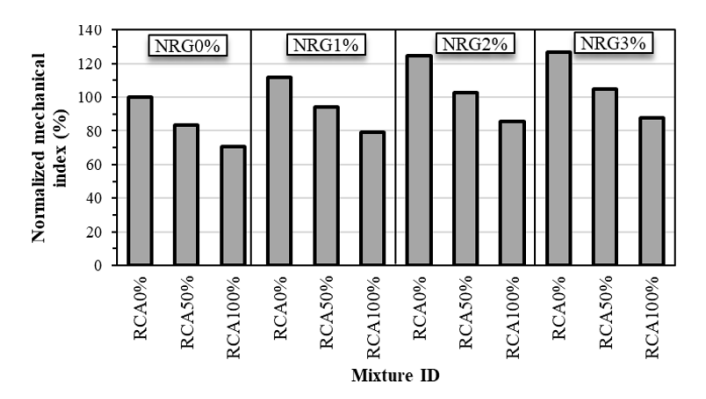


Figure 14. Normalized mechanical index

The presented behavior reveals a distinct stratification among SCC-NGRA mixtures incorporating RCA, NRG, or their combination. Mixtures containing only RCA showed markedly reduced performance. Notably, the 100% RCA mixture yielded the lowest index (70.4%), followed by 50% RCA at 83.3%, confirming that higher substitution levels of with RCA diminish matrix continuity microstructural cohesion. This degradation is consistent with the findings of Etxeberria et al. [67], who reported that RCA weakens the ITZ and increases porosity in SCC matrices. In contrast, mixtures incorporating NRG demonstrated significant performance enhancement. The 3% NRG mixture achieved the highest NMI (126.7%), with 2% NRG closely behind at 124.7%, clearly surpassing the control. These improvements are attributed to the pozzolanic reactivity and filler effect of NRG, which promote matrix densification and secondary CSH formation. Similar enhancements have been documented for nano-silica systems in SCC by the study [65]. Mixtures combining RCA and NRG exhibited intermediate performance. For instance, the inclusion of 1% NRG raised the 100% NMI of **RCA** from 70.4% (100%RCA1%NRG), while 3% NRG increased it further to 87.7% (100%RCA3%NRG). This suggests that NRG can partially mitigate the mechanical drawbacks of RCA, though the improvement is proportional to the NRG dosage and does not fully restore strength to control levels.

It is also noteworthy that NRG enriched mixtures exhibited relatively higher improvements in flexural strength than in direct tensile strength, highlighting NRG's stronger influence on crack bridging, post peak ductility, and energy absorption. This observation is in agreement with earlier findings in Section 3.2. In addition, a comparable enhancement in flexural performance was reported by Ahmed et al. [68], who demonstrated that incorporating nano-silica into lightweight structural concrete mixtures significantly improved flexural strength. This improvement was attributed to the densification of the cement matrix and enhanced microstructural integrity, even when utilizing RA.

7. CONCLUSION

This study investigated the influence of NRG and RCA on the performance of sustainable SCC-NGRA mixtures. Through a comprehensive experimental program, key mechanical and rheological characteristics were examined in relation to varying replacement levels. The findings contribute meaningful insights into the feasibility of integrating industrial waste into structural concrete while maintaining required performance standards. Drawing on the outcomes of this study, the following conclusions are presented:

- (1) Incorporation of NRG as a cement replacement up to 3% by weight enhanced compressive strength and reduced the environmental footprint of concrete, confirming its potential as a high-performance pozzolanic additive derived from recycled glass waste.
- (2) The combined use of RCA and NRG exhibited complementary effects on workability and strength, supporting the feasibility of producing SCC-NGRA with high recycled content.
- (3) Fresh-state performance was strongly influenced by RCA content, where higher replacement reduced flowability. This effect was partially mitigated by the fine particle packing and surface reactivity of NRG, which improved cohesion and viscosity.
- (4) Mechanical properties, particularly splitting tensile and flexural strengths, showed moderate enhancement at lower NRG dosages, suggesting improved microstructural integrity through pozzolanic densification and refined pore structure.
- (5) Durability-related benefits, though not the primary scope of this study, are implied through reduced porosity and denser ITZs observed in mixtures with NRG. Further investigation into long-term durability is therefore recommended.
- (6) This work contributes a novel approach to zero-waste concrete design, providing practical insights for sustainable construction by valorizing both demolition-derived coarse aggregates and post-consumer glass, in line with the sustainable development goals of the construction sector.

REFERENCES

- [1] Ramachandran, V.S. (1981). Waste and by-products as concrete aggregates. Canadian Building Digest, 215. https://doi.org/10.4224/40000747
- [2] Ahmadi, B., Al-Khaja, W. (2001). Utilization of paper waste sludge in the building construction industry. Resources, Conservation and Recycling, 32(2): 105-113. https://doi.org/10.1016/S0921-3449(01)00051-9
- [3] Zhang, T., Chen, M., Wang, Y., Zhang, M. (2023). Roles of carbonated recycled fines and aggregates in hydration, microstructure and mechanical properties of concrete: A critical review. Cement and Concrete Composites, 138: 104994.
 - https://doi.org/10.1016/j.cemconcomp.2023.104994
- [4] Shi, X., Mukhopadhyay, A., Zollinger, D., Grasley, Z. (2019). Economic input-output life cycle assessment of concrete pavement containing recycled concrete aggregate. Journal of Cleaner Production, 225: 414-425. https://doi.org/10.1016/j.jclepro.2019.03.288
- [5] Kaza, S., Yao, L.C., Bhada-Tata, P., Van Woerden, F. (2018). What a waste 2.0: A global snapshot of solid waste management to 2050. World Bank Publications.

- https://doi.org/10.1596/978-1-4648-1329-0
- [6] Kumari, S., Agarwal, S., Khan, S. (2022). Micro/nano glass pollution as an emerging pollutant in near future. Journal of Hazardous Materials Advances, 6: 100063. https://doi.org/10.1016/j.hazadv.2022.100063
- [7] Zhong, R., Leng, Z., Poon, C.S. (2018). Research and application of pervious concrete as a sustainable pavement material: A state-of-the-art and state-of-the-practice review. Construction and Building Materials, 183: 544-553. https://doi.org/10.1016/j.conbuildmat.2018.06.131
- [8] He, C.H., Liu, H.W., Liu, C. (2024). A fractal-based approach to the mechanical properties of recycled aggregate concretes. Facta Universitatis, Series: Mechanical Engineering, 22(2): 329-342. https://doi.org/10.22190/FUME240605035H
- [9] Shariat, M., Shariati, M., Madadi, A., Wakil, K. (2018). Computational Lagrangian Multiplier Method by using for optimization and sensitivity analysis of rectangular reinforced concrete beams. Steel and Composite Structures, 29(2): 243-256. https://doi.org/10.12989/scs.2018.29.2.243
- [10] Raki, L., Beaudoin, J., Alizadeh, R., Makar, J., Sato, T. (2010). Cement and concrete nanoscience and nanotechnology. Materials, 3(2): 918-942. https://doi.org/10.3390/ma3020918
- [11] Aljumaili, M.W., Beddu, S.B., Itam, Z., Their, J.M. (2024). Investigating the influence of recycled coarse aggregate and steel fiber on the rheological and mechanical properties of self-compacting geopolymer concrete. Annales de Chimie Science des Matériaux, 48(2): 197-206. https://doi.org/10.18280/acsm.480206
- [12] Parthiban, K., Mohan, K.S.R. (2017). Influence of recycled concrete aggregates on the engineering and durability properties of alkali activated slag concrete. Construction and Building Materials, 133: 65-72. https://doi.org/10.1016/j.conbuildmat.2016.12.050
- [13] Xie, J., Wang, J., Zhang, B., Fang, C., Li, L. (2019). Physicochemical properties of alkali activated GGBS and fly ash geopolymeric recycled concrete. Construction and Building Materials, 204: 384-398. https://doi.org/10.1016/j.conbuildmat.2019.01.286
- [14] Aljumaili, M.W., Beddu, S., Itam, Z., Their, J.M. (2024). Mechanical characteristics and durability of metakaolin-based self-compacting geopolymer concrete as a function of recycled aggregate and steel fiber contents. Journal of Composite & Advanced Materials / Revue des Composites et des Matériaux Avancés, 34(4): 465-480. https://doi.org/10.18280/rcma.340408
- [15] Sobuz, M.H.R., Saha, A., Akid, A.S.M., Vincent, T., Tam, V.W.Y., Yalçınkaya, Ç., Mujahid, R., Sutan, N.M. (2023). Performance of self-compacting concrete incorporating waste glass as coarse aggregate. Journal of Sustainable Cement-Based Materials, 12(5): 527-541. https://doi.org/10.1080/21650373.2022.2086936
- [16] Lu, J.X., Poon, C.S. (2018). Improvement of early-age properties for glass-cement mortar by adding nanosilica. Cement and Concrete Composites, 89: 18-30. https://doi.org/10.1016/j.cemconcomp.2018.02.010
- [17] Lee, H., Hanif, A., Usman, M., Sim, J., Oh, H. (2018). Performance evaluation of concrete incorporating glass powder and glass sludge wastes as supplementary cementing material. Journal of Cleaner Production, 170: 683-693. https://doi.org/10.1016/j.jclepro.2017.09.233

- [18] Omran, A., Tagnit-Hamou, A. (2016). Performance of glass-powder concrete in field applications. Construction and Building Materials, 109: 84-95. https://doi.org/10.1016/j.conbuildmat.2016.02.006
- [19] Jochem, L.F., Casagrande, C.A., Onghero, L., Venancio, C., Gleize, P.J. (2021). Effect of partial replacement of the cement by glass waste on cementitious pastes. Construction and Building Materials, 273: 121704. https://doi.org/10.1016/j.conbuildmat.2020.121704
- [20] Aliabdo, A.A., Abd Elmoaty, M.E.M., Aboshama, A.Y. (2016). Utilization of waste glass powder in the production of cement and concrete. Construction and Building Materials, 124: 866-877. https://doi.org/10.1016/j.conbuildmat.2016.08.016
- [21] Poudel, S., Bhetuwal, U., Kharel, P., Khatiwada, S., KC, D., Dhital, S., Suman, S. (2025). Waste glass as partial cement replacement in sustainable concrete: Mechanical and fresh properties review. Buildings, 15(6): 857. https://doi.org/10.3390/buildings15060857
- [22] Sobuz, M.H.R., Meraz, M.M., Safayet, M.A., Mim, N.J., Mehedi, M.T., Farsangi, E.N., Meraz, M.M. (2023). Performance evaluation of high-performance selfcompacting concrete with waste glass aggregate and metakaolin. Journal of Building Engineering, 67: 105976. https://doi.org/10.1016/j.jobe.2023.105976
- [23] Dahamm, E.K., Hama, S.M., Al-Jumaily, I.A. (2023). Effect of nano-sized clay and waste glass powder on rheological and hardened properties of self-compacting concrete. Research on Engineering Structures and Materials, 9(3): 743-761. https://doi.org/10.17515/resm2022.563ma1026
- [24] Onaizi, A.M.A.S. (2022). Enhancement of mechanical properties of high-volume fly ash concrete using glass nano powder and effective microorganisms. Universiti Teknologi Malaysia. https://doi.org/10.13140/RG.2.2.25183.33443
- [25] Cai, Y., Xuan, D., Poon, C.S. (2019). Effects of nano-SiO₂ and glass powder on mitigating alkali-silica reaction of cement glass mortars. Construction and Building Materials, 201: 295-302. https://doi.org/10.1016/j.conbuildmat.2018.12.186
- [26] Zhao, Y., Meng, B., Yin, X., Bao, Y. (2024). The sustainable use of waste glass powder in concrete-filled steel tubes: A mechanical and economic analysis. Buildings, 14(12): 3892. https://doi.org/10.3390/buildings14123892
- [27] Onaizi, A.M.A.S., Lim, N.H.A.S., Huseien, G.F., Amran, M., Ma, C.K. (2022). Effect of the addition of nano glass powder on the compressive strength of highvolume fly ash modified concrete. Materials Today: Proceedings, 48(6): 1789-1795. https://doi.org/10.1016/j.matpr.2021.08.347
- [28] Zhao, H., Li, W., Gan, Y., Mahmood, A.H., Zhao, X., Wang, K. (2024). Nano-and microscopic investigation on the strengthening mechanism of ITZs using waste glass powder in modeled aggregate concrete. Journal of Materials in Civil Engineering, 36(4): 04024007. https://doi.org/10.1061/JMCEE7.MTENG-16956
- [29] Ayub, T., Jamil, T., Ayub, A., Khan, A.U.R., Mehmood, E., Sheikh, M.D. (2024). Effect of glass powder on the compressive strength and drying shrinkage behavior of OPC-and LC3-50-based cementitious composites of various strengths. Advances in Materials Science and Engineering, 2024(1): 8860083.

- https://doi.org/10.1155/2024/8860083
- [30] Grdić, D.Z., Topličić-Ćurčić, G.A., Grdić, Z.J., Ristić, N.S. (2021). Durability properties of concrete supplemented with recycled CRT glass as cementitious material. Materials, 14(16): 4421. https://doi.org/10.3390/ma14164421
- [31] Tuaum, A., Shitote, S., Oyawa, W. (2018). Experimental study of self-compacting mortar incorporating recycled glass aggregate. Buildings, 8(2): 15. https://doi.org/10.3390/buildings8020015
- [32] Zhu, W., Bartos, P.J.M. (2003). Permeation properties of self-compacting concrete. Cement and Concrete Research, 33(6): 921-926. https://doi.org/10.1016/S0008-8846(02)01090-6
- [33] You, Z., Mills-Beale, J., Foley, J.M., Roy, S., Odegard, G.M., Dai, Q., Goh, S.W. (2011). Nanoclay-modified asphalt materials: Preparation and characterization. Construction and Building Materials, 25(2): 1072-1078. https://doi.org/10.1016/j.conbuildmat.2010.06.070
- [34] Gong, K., White, C.E. (2023). Development of physics-based compositional parameters for predicting the reactivity of amorphous aluminosilicates in alkaline environments. Cement and Concrete Research, 174: 107296 https://doi.org/10.1016/j.cemconres.2023.107296
- [35] Curcio, A., Sabato, A.G., Nunez Eroles, M., Gonzalez-Rosillo, J.C., Morata, A., Tarancon, A., Ciucci, F. (2022). Ultrafast crystallization and sintering of Li_{1.5}Al_{0.5}Ge_{1.5}(PO₄)₃ glass and its impact on ion conduction. ACS Applied Energy Materials, 5(11): 14466-14475. https://doi.org/10.1021/acsaem.2c03009
- [36] Ahari, R.S., Erdem, T.K., Ramyar, K. (2015). Effect of various supplementary cementitious materials on rheological properties of self-consolidating concrete. Construction and Building Materials, 75: 89-98. https://doi.org/10.1016/j.conbuildmat.2014.11.014
- [37] Mohammed, A.M., Asaad, D.S., Al-Hadithi, A.I. (2022). Experimental and statistical evaluation of rheological properties of self-compacting concrete containing fly ash and ground granulated blast furnace slag. Journal of King Saud University Engineering Sciences, 34(6): 388-397. https://doi.org/10.1016/j.jksues.2020.12.005
- [38] ASTM International. (2021). ASTM C39/C39M-21: Standard Test Method for Compressive Strength of Cylindrical Concrete Specimens. ASTM International, West Conshohocken, PA, USA.
- [39] ASTM International. (2011). ASTM C496/C496M-11: Standard Test Method for Splitting Tensile Strength of Cylindrical Concrete Specimens. ASTM International, West Conshohocken, PA. https://doi.org/10.1520/C0496 C0496M-11
- [40] Morshedian, M. (1995). ASTM C78–C78M, ACI Struct. Iranian Journal of Polymer Science and Technology, 4: 1-7.
- [41] Nemocón, S.A.G., Marriaga, J.M.L., Suárez, J.D.P. (2022). Rheological and hardened properties of selfcompacting concrete using hollow glass microspheres as a partial replacement of cement. Construction and Building Materials, 342: 128012. https://doi.org/10.1016/j.conbuildmat.2022.128012
- [42] Harbouz, I., Yahia, A., Roziere, E., Loukili, A. (2023). Printing quality control of cement-based materials under flow and rest conditions. Cement and Concrete Composites, 138: 104965.

- https://doi.org/10.1016/j.cemconcomp.2023.104965
- [43] British Standard, E.N. (2016). 206, Concrete Specifications, Performance, Production and Conformity. BSI, London.
- [44] Güneyisi, E., Gesoglu, M., Algin, Z., Yazıcı, H. (2016). Rheological and fresh properties of self-compacting concretes containing coarse and fine recycled concrete aggregates. Construction and Building Materials, 113: 622-630.
 - https://doi.org/10.1016/j.conbuildmat.2016.03.073
- [45] Assaad, J.J., Khayat, K.H. (2006). Effect of viscosity-enhancing admixtures on formwork pressure and thixotropy of self-consolidating concrete. ACI Materials Journal, 103(4): 280-287. https://doi.org/10.14359/16612
- [46] Zhang, C., Nerella, V.N., Krishna, A., Wang, S., Zhang, Y. (2021). Mix design concepts for 3D printable concrete: A review. Cement and Concrete Composites, 122: 104155. https://doi.org/10.1016/j.cemconcomp.2021.104155
- [47] Mohseni, E., Kazemi, M.J., Koushkbaghi, M., Zehtab, B., Behforouz, B. (2019). Evaluation of mechanical and durability properties of fiber-reinforced lightweight geopolymer composites based on rice husk ash and nanoalumina. Construction and Building Materials, 209: 532-540. https://doi.org/10.1016/j.conbuildmat.2019.03.067
- [48] Liu, Y., Chen, S.J., Sagoe-Crentsil, K., Duan, W. (2021). Digital concrete modelling: An alternative approach to microstructural pore analysis of cement hydrates. Construction and Building Materials, 303: 124558. https://doi.org/10.1016/j.conbuildmat.2021.124558
- [49] Altayawı, O.A.A., Öz, H.Ö., Mermerdaş, K. (2023). Using of thermal power plant fly ash to produce semilightweight aggregate and concrete. Sigma Journal of Engineering and Natural Sciences, 41(1): 42-48. https://doi.org/10.14744/sigma.2023.00005
- [50] Wang, J., Che, Z., Zhang, K., Fan, Y., Niu, D., Guan, X. (2023). Performance of recycled aggregate concrete with supplementary cementitious materials (fly ash, GBFS, silica fume, and metakaolin): Mechanical properties, pore structure, and water absorption. Construction and Building Materials, 368: 130455. https://doi.org/10.1016/j.conbuildmat.2023.130455
- [51] Shi, C., Wu, Y., Riefler, C., Wang, H. (2005). Characteristics and pozzolanic reactivity of glass powders. Cement and Concrete Research, 35(5): 987-993. https://doi.org/10.1016/j.cemconres.2004.06.024
- [52] Jo, B.W., Kim, C.H., Tae, G.H., Park, J.B. (2007). Characteristics of cement mortar with nano-SiO₂ particles. Construction and Building Materials, 21(6): 1351-1355. https://doi.org/10.1016/j.conbuildmat.2005.12.020
- [53] American Concrete Institute (2011). ACI 214R-11: Guide to evaluation of strength test results of concrete. American Concrete Institute, Farmington Hills, MI, USA.
- [54] Kou, S.C., Poon, C.S. (2012). Enhancing the durability properties of concrete prepared with coarse recycled aggregate. Construction and Building Materials, 35: 69-76. https://doi.org/10.1016/j.conbuildmat.2012.02.022
- [55] Alibeigibeni, A., Stochino, F., Zucca, M. (2025). Enhancing concrete sustainability: A critical review of the performance of recycled concrete aggregates (RCAs) in structural concrete. Buildings, 15(8): 1-25.

- https://doi.org/10.3390/buildings15081361
- [56] Rahmawati, C., Aprilia, S., Saidi, T., Aulia, T.B., Hadi, A.E. (2021). The effects of nanosilica on mechanical properties and fracture toughness of geopolymer cement. Polymers, 13(13): 2178. https://doi.org/10.3390/polym13132178
- [57] Raza, S.S., Fahad, M., Ali, B., Amir, M.T., Alashker, Y., Elhag, A.B. (2022). Enhancing the performance of recycled aggregate concrete using micro-carbon fiber and secondary binding material. Sustainability, 14(21): 14613. https://doi.org/10.3390/su142114613
- [58] Ali, T., Qureshi, M.Z., Onyelowe, K.C., Althaqafi, E., Deifalla, A., Ahmed, H., Ajwad, A. (2025). Optimizing recycled aggregate concrete performance with chemically and mechanically activated fly ash in combination with coconut fiber. Scientific Reports, 15(1): 9346. https://doi.org/10.1038/s41598-025-92227-x
- [59] Ashraf, M.J., Idrees, M., Akbar, A. (2023). Performance of silica fume slurry treated recycled aggregate concrete reinforced with carbon fibers. Journal of Building Engineering, 66: 105892. https://doi.org/10.1016/j.jobe.2023.105892
- [60] Ferrara, L., Krelani, V., Carsana, M. (2014). A "fracture testing" based approach to assess crack healing of concrete with and without crystalline admixtures. Construction and Building Materials, 68: 535-551. https://doi.org/10.1016/j.conbuildmat.2014.07.008
- [61] Safiuddin, M., Alengaram, U.J., Rahman, M.M., Salam, M.A., Jumaat, M.Z. (2013). Use of recycled concrete aggregate in concrete: A review. Journal of Civil Engineering and Management, 19(6): 796-810. https://doi.org/10.3846/13923730.2013.799093
- [62] Aygün, B.F. (2021). An Overview of the impact of using

- glass powder on mechanical, durability properties in self-compacting concrete. Journal of Sustainable Construction Materials and Technologies, 6(3): 116-123. https://doi.org/10.29187/jscmt.2021.67
- [63] Silva, R.V., De Brito, J., Dhir, R.K. (2016). Establishing a relationship between modulus of elasticity and compressive strength of recycled aggregate concrete. Journal of Cleaner Production, 112: 2171-2186. https://doi.org/10.1016/j.jclepro.2015.10.064
- [64] Şahmaran, M., Yaman, İ.Ö., Tokyay, M. (2009). Transport and mechanical properties of self-consolidating concrete with high volume fly ash. Cement and Concrete Composites, 31(2): 99-106. https://doi.org/10.1016/j.cemconcomp.2008.12.003
- [65] Mustapha, F.A., Sulaiman, A., Mohamed, R.N., Umara, S.A. (2021). The effect of fly ash and silica fume on self-compacting high-performance concrete. Materials Today: Proceedings, 39: 965-969. https://doi.org/10.1016/j.matpr.2020.04.493
- [66] Li, H., Zhang, M.H., Ou, J.P. (2007). Flexural fatigue performance of concrete containing nano-particles for pavement. International Journal of Fatigue, 29(7): 1292-1301. https://doi.org/10.1016/j.ijfatigue.2006.10.004
- [67] Etxeberria, M., Vázquez, E., Marí, A., Barra, M. (2007). Influence of amount of recycled coarse aggregates and production process on properties of recycled aggregate concrete. Cement and Concrete Research, 37(5): 735-742. https://doi.org/10.1016/j.cemconres.2007.02.002
- [68] Ahmed, S.A.G., Ebrahem, E., El-Feky, M.S. (2024). Achieving sustainable performance: Synergistic effects of nano-silica and recycled expanded polystyrene in lightweight structural concrete. Scientific Reports, 14(1): 26648. https://doi.org/10.1038/s41598-024-77029-x